World Journal of Biology Pharmacy and Health Sciences
eISSN: 2582-5542
Cross Ref DOI: 10.30574/wjbphs
Journal homepage: https://wjbphs.com/

(CASE REPORT)

Check for updates

Double outlet right ventricle accompanied by complex congenital anomalies: A rare association

Akhil Mehrotra *, Faiz Illahi Siddiqui and Mohammad Shaban

Prakash Heart Station, Nirala Nagar, Lucknow, UP, India, 226020.

World Journal of Biology Pharmacy and Health Sciences, 2024, 18(03), 199–215

Publication history: Received on 26 April 2024; revised on 10 June 2024; accepted on 13 June 2024

Article DOI: https://doi.org/10.30574/wjbphs.2024.18.3.0332

Abstract

Double outlet right ventricle (DORV) comprises a heterogeneous series of associated cardiac anomalies that involve the RV outflow tract in which both of the great arteries arise entirely or predominantly from the RV. The anatomic dysmorphology is variable, and there may be associated cardiac anomalies.

We report here a case of a complex cyanotic heart disease in a 14 year old adolescent comprising of DORV accompanied by multiple congenital cardiac anomalies: single atrium, complete AV canal defect, severe AV valve regurgitation, D-malposition of great arteries, subaortic obstruction and pulmonary valvular stenosis.

Keywords: DORV; Single atrium; Remote VSD; Atrioventricular septal defect; Pulmonary stenosis; Subaortic stenosis; Subaortic membrane; Subpulmonic conus

1. Introduction

The term “double outlet right ventricle" refers to a family of anatomically related complex congenital cardiac lesions involving the outflow tracts. DORV anatomy was first described by Mery in 1703 [1]. More than 200 years later, the term "double-outlet ventricle" was employed by Braun et al [2] in 1952. Shortly thereafter, Witham described "double outlet right ventricle" as a specific cardiac diagnosis [3]. In 1972, Lev et al [4] used the relationship of the VSD to the great arteries as the basis for his classification. Van Praagh et al [5] and Peixoto et al [6] developed the most noteworthy classification schemes applied to DORV (Tables 1, 2; Figures 1, 2).

Table 1 DORV categories based on VSD location and the relationship with great arteries [6]

Subaortic VSD
Subpulmonary VSD
Doubly committed VSD
Non-committed VSD/remote VSD

Table 2 DORV categories based on great vessel relationship [6]

Right anterior aorta	Left anterior aorta
Right posterior aorta	Left posterior aorta
Right lateral/side-by-side aorta	

* Corresponding author: Akhil Mehrotra

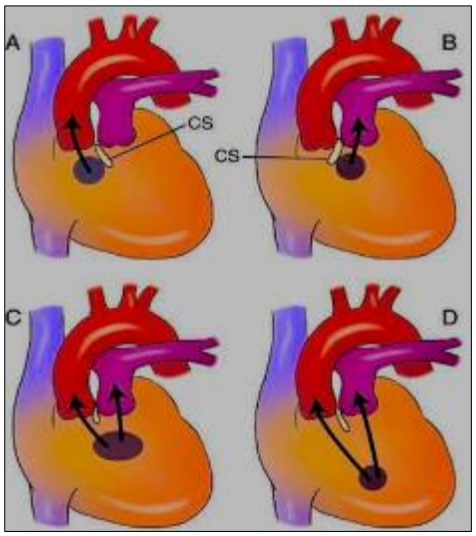

Figure 1 Diagram of the four types of VSD that occur in DORV [6]. (A), Subaortic VSD; note the anterior and leftward deviation of the conal septum (CS), causing the aorta to override the VSD and the subpulmonary region to be narrowed. (B), Subpulmonary VSD; note the posterior and rightward deviation of the conal septum, resulting in the pulmonary artery overriding the VSD and subaortic narrowing. (C), Doubly committed VSD; the conal septum is absent and the VSD is large. (D), Remote or noncommitted VSD in the muscular septum

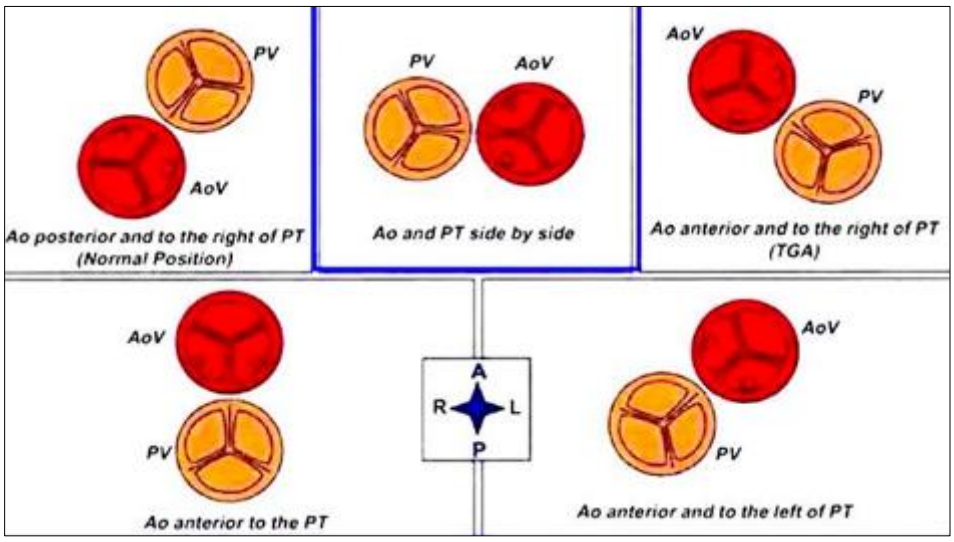

Figure 2 DORV categories based on great vessel relationships [6]. Illustration of the echocardiographic view of the spatial relationship of the semilunar cusps in hearts with DORV in a parasternal cross section. A-anterior; Ao-aorta; R-right; L-left; P-posterior; TGA-transposition of the great arteries; PT-pulmonary trunk; AoV-aortic valve; PV-pulmonary valve

Walters et al [7], mentioned that some authors used the degree of aortic override as a defining criterion for the diagnosis of DORV such that if the aorta is more than 50% over the right ventricle, it is labelled DORV. This “50% rule" becomes problematic in cases of tetralogy of Fallot with extreme override of the aorta. Alternatively, the absence or loss of normal fibrous continuity between the mitral and aortic valves (that is, presence of subaortic conus) has been proposed as a definition of DORV. This, too, is problematic as the presence of subaortic conus is a continuous variable in DORV and one that does not lend itself to a binary or dichotomous definition [7]. The Congenital Heart Surgery Nomenclature and Database Project was developed to provide a more unified and inclusive framework for classification of congenital heart disease and assessment of surgical repair [7]. The consensus definition of DORV was made deliberately broad by stating "DORV is a type of ventriculoarterial connection in which both great vessels arise either entirely or predominantly from the right ventricle". Consistent with other complex CHDs, DORV may occur as an isolated cardiac defect, together with

other cardiac lesions, or in association with extracardiac anomalies [1, 8-14]. It occurs in approximately 3-9/100 000 live births [15-17] although at least one report noted rates of between 15-24/100 000 [18]. Conservative estimates project DORV accounting for about 1-3% of all congenital heart defects [15, 19].

Cardiac CT offers higher image quality and accessibility due to high spatial resolution and short scan time [20-22]. Three-dimensional (3D) printing technology has recently been used to characterize the morphologic details of DORV (Figures 3-7) [23-26]. Because the quality of source images determines the quality of 3D-printed heart models, cardiac CT is the most commonly used imaging modality in 3D printing for congenital heart disease [27].

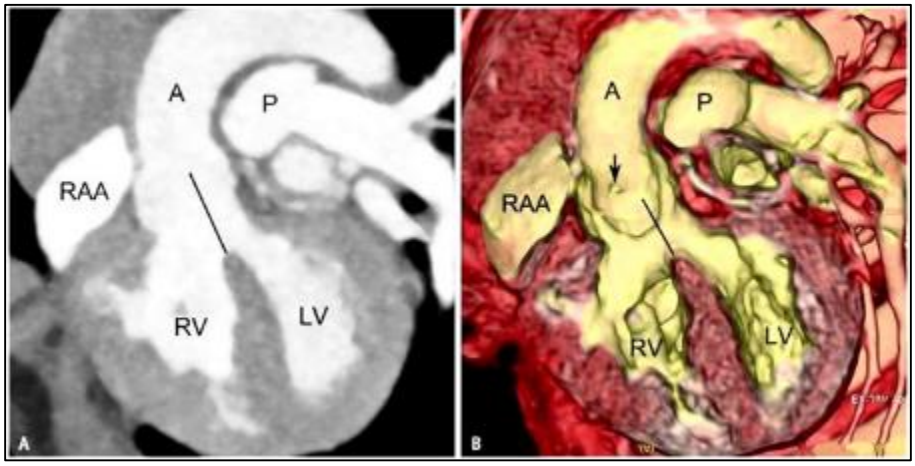

Figure 3 *Practical 50% rule in a neonate with double outlet RV with subaortic ventricular septal defect and pulmonary stenosis.* A, B. Long-axis CT image (A) and transparent-lumen volume-rendered CT image (B) show that a diameter > 50% of the annulus of the overriding aortic valve is connected to the morphologic RV based on an extension line of the ventricular septum. In clinical practice, measuring the diameter is more frequently used than the original method for measuring the circumference. The origin of the right coronary artery (arrow in B) was noted. A = aorta, LV = left ventricle, P = pulmonary artery, RAA = right atrial appendage, RV = right ventricle

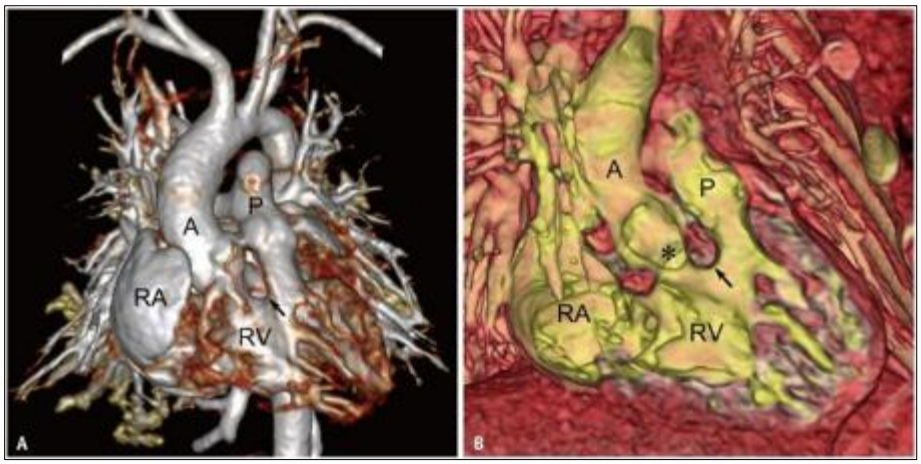

Figure 4 *Double outlet RV with subaortic VSD in a neonate.* A, B. Standard (A) and transparent-lumen (B) volume-rendered CT images show that P is exclusively connected to the RV, and more than half of the A is connected to the RV. The outlet septum (arrows) is fused with the anterior margin of the subaortic VSD (asterisk). A = ascending aorta, P= pulmonary artery, RA = right atrium, RV = right ventricle, VSD = ventricular septal defect

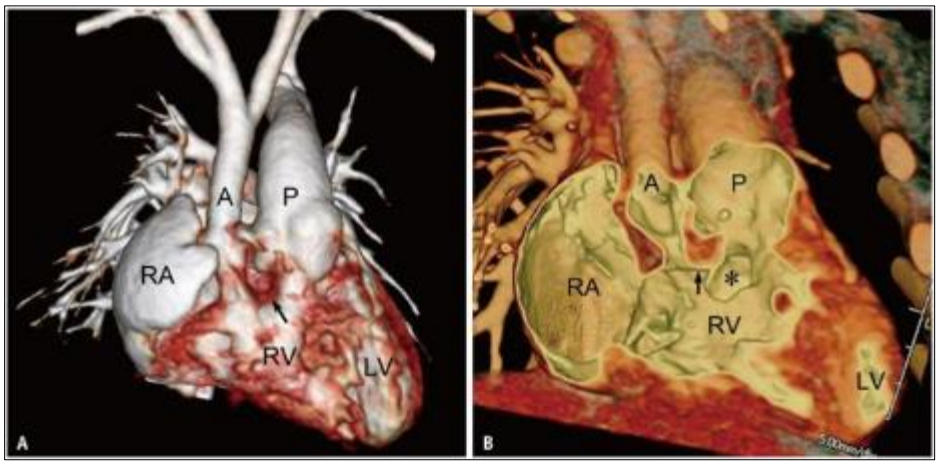

Figure 5 *Double outlet RV with subpulmonary VSD in a neonate.* A, B. Standard (A) and transparent-lumen (B) volume-rendered CT images show that both great arteries are connected to the morphologic RV. The outlet septum (arrows) is fused with the posterior margin of the subpulmonary VSD (asterisk). A is relatively small, and subaortic stenosis is observed. In addition, coarctation of the aorta was observed in this patient (not shown). A = ascending aorta, LV = left ventricle, P = pulmonary artery, RA = right atrium, RV right ventricle, VSD = ventricular septal defect

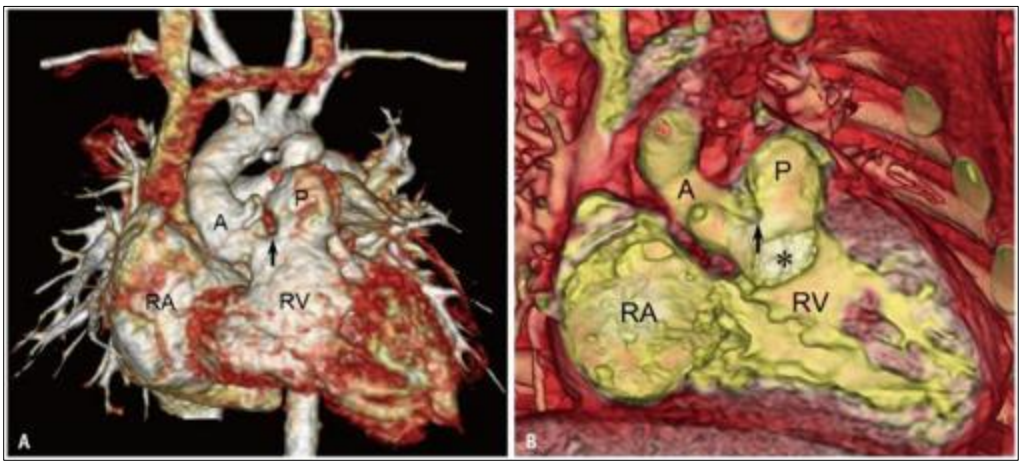

Figure 6 *Double outlet RV with doubly-committed VSD in an infant.* A, B. Standard (A) and transparent-lumen (B) volume-rendered CT images show that both great arteries are connected to the morphologic RV. The outlet septum (arrows) is fibrous, characteristic of a doubly committed VSD (asterisk). A = ascending aorta, P = pulmonary artery, RA = right atrium, RV = right ventricle, VSD = ventricular septal defect

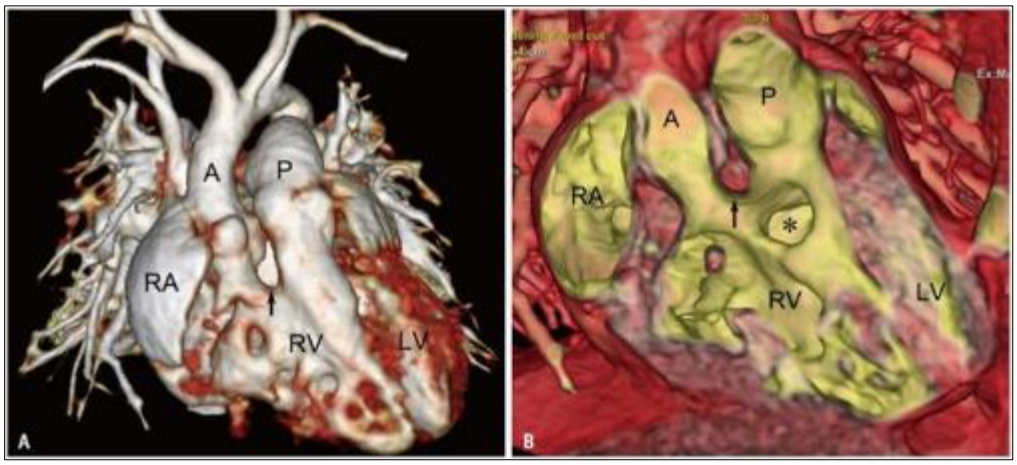

Figure 7 *Double outlet RV with non-committed VSD in a neonate.* A, B. Standard (A) and transparent-lumen (B) volume-rendered CT images show that both great arteries are connected to the morphologic RV. The non-committed VSD (asterisk) is far from both arterial valves but closer to the pulmonary valve than the aortic valve. The muscular outlet septum (arrows) is noted. A = ascending aorta, LV = left ventricle, P = pulmonary artery, RA = right atrium, RV = right ventricle, VSD = ventricular septal defect

2. Case Report

A 14 year old adolescent male presented to us with severe breathlessness, central cyanosis and congestive heart failure (Figure 8).

On clinical examination, the patient was of average built with marked central cyanosis and conspicuous clubbing of the tips of all the fingers and toes. Moreover, the patient was having gross congestive heart failure including ashen colored face, facial puffiness, orthopnea, swelling of the abdomen and feet. His weight was 46 kg, pulse rate was 85/min, BP was 90/70 mmHg, SPO2 was 72% at room air, respiratory rate was 28/min. There was striking protruding chest wall deformity present. All the peripheral pulses were normally palpable without any radio femoral delay.

On cardiovascular examination, there was Grade III/IV ejection systolic murmur heard in the pulmonary area and Grade IV/VI pansytolic murmur over the apex. The first heart sound was normal and the second heart sound was widely split. There was no clicks or gallop sound heard.

While examining the respiratory system there was bilateral basal stony dullness on percussion and on auscultation there was diminution of breath sounds, perhaps due to bilateral pleural effusion. Furthermore, on abdominal examination, significant ascites was present alongwith moderate hepatomegaly (Liver was 7-10 cm enlarged, on palpation of the right hypochondrium. It was firm and tender). Rest of the systemic examination was unremarkable

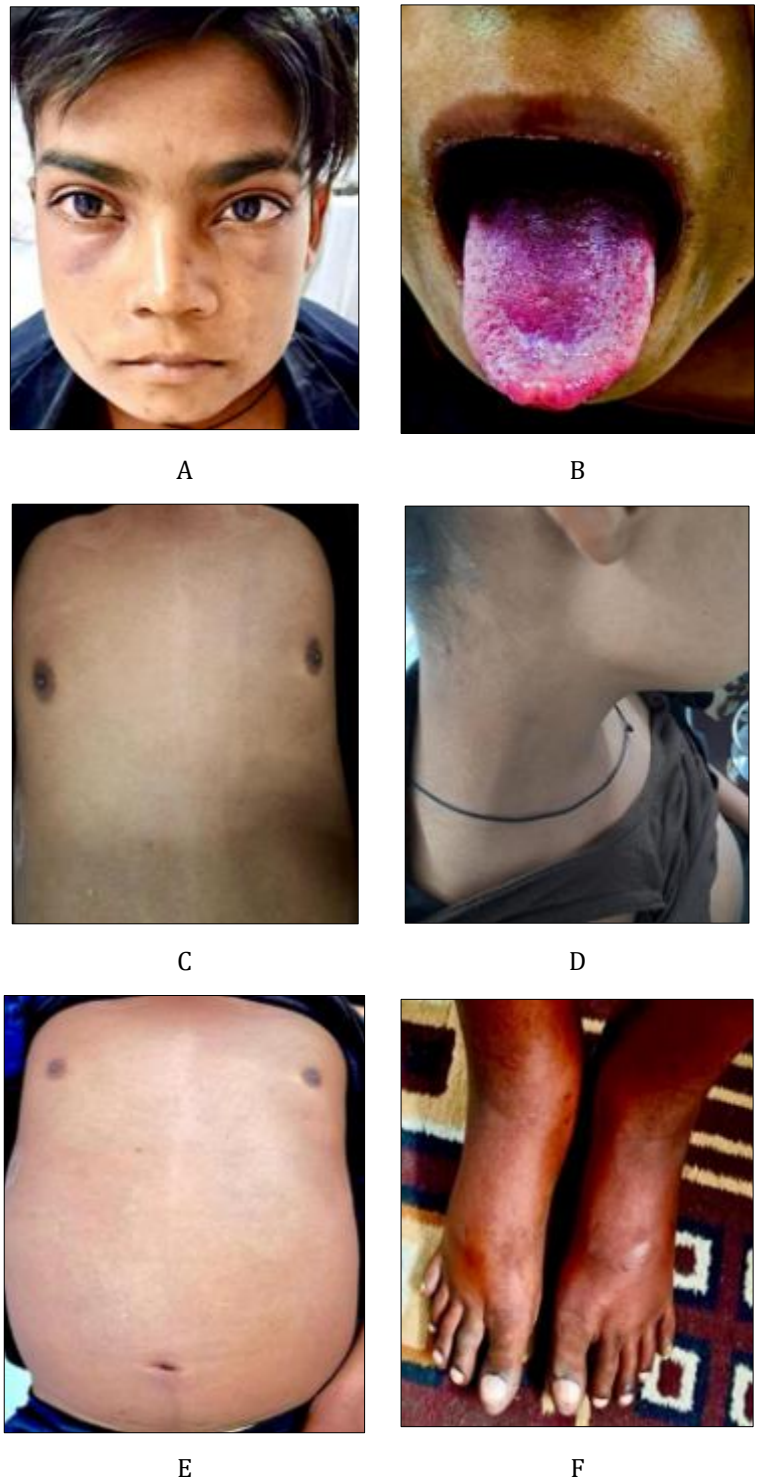

Figure 8 (A) Facial features indicate puffiness below both lower eyelids, congestion of conjunctiva and bluish colouration of lips. (B) deep cyanosis of tongue; (C) protuberant chest wall deformity; (D) jugular venous distension present; (E) notable ascites was present; (F) gross pedal edema with clubbing of toes

Xray chest (PA) depicts considerable cardiomegaly with reduced pulmonary blood flow(Figure 9).

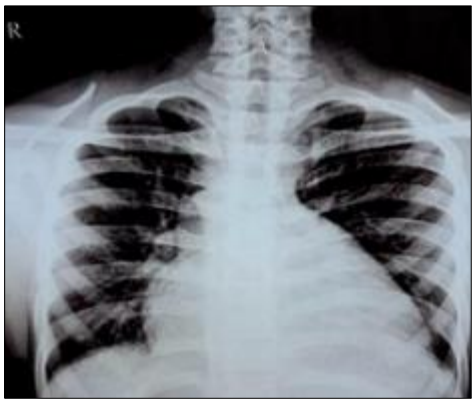

Figure 9 X-ray chest (PA) view. There is considerable cardiomegaly with diminished pulmonary blood flow

Resting ECG shows first degree A-V block with a PR interval of 275 msec, normal sinus rhythm with a ventricular rate of 78/min, right ventricular hypertrophy and extreme left axis deviation (Figure 10).

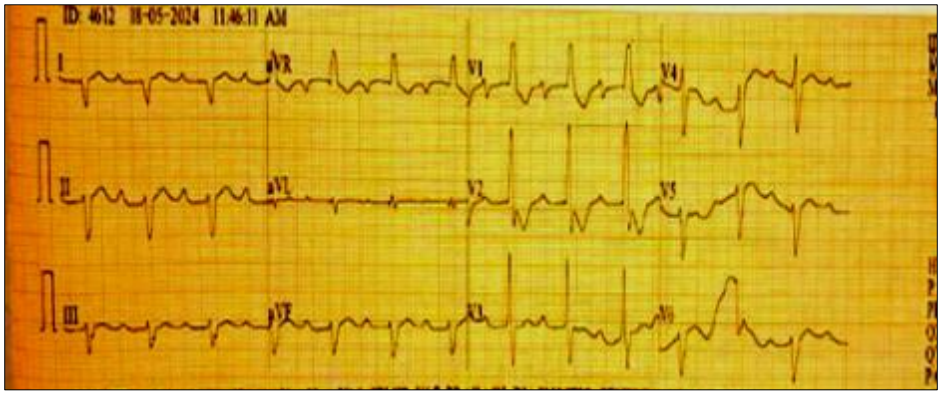

Figure 10 Resting ECG illustrates first degree A-V block with a PR interval 275 msec, normal sinus rhythm with a ventricular rate of 78/min, right ventricular hypertrophy and extreme left axis deviation

2.1. Transthoracic Echocardiography

All echocardiography evaluations were performed by the author, using My Lab X7 4D XStrain echocardiography machine, Esaote, Italy. The images were acquired using a adult probe equipped with harmonic variable frequency electronic single crystal array transducer while the subject was lying in supine and left lateral decubitus positions.

Conventional M-mode, two-dimensional and pulse wave doppler (PWD) and continuous wave doppler (CWD) echocardiography was performed in the classical subcostal, parasternal long axis (LX), parasternal short axis (SX), 4-Chamber (4CH), 5-Chamber (5CH) and suprasternal views. Contemporary sequential segmental approach for echocardiographic analysis of our index patient was accomplished and the characteristic features were depicted (Figures 11-18).

2.2. M-Mode Echocardiography

M-mode echocardiography of right and left ventricle was performed and the estimated measurements are outlined.

Table 3 Calculations of M-mode echocardiography

Measurements	RV	LV
IVS d	7.3 mm	8.0 mm
LVID d	57.8 mm	23.3 mm
LVPW d	9.6 mm	7.3 mm
IVS s	13.4 mm	10.7 mm
LVID s	40.9 mm	18.7 mm
LVPW s	14.2 mm	9.2 mm
EF	55 %	43 %
%LVFS	29 %	20 %
LVEDV	165.0 ml	18.8 ml
LVESV	73.9 ml	10.8 ml
SV	91.1 ml	8.0 ml
LV Mass	186 g	38 g

2.3. Summary of M-mode echocardiography

The RV was dilated with concentric hypertrophy and normal systolic function - RVEF 55%. RV mass was 186g. Conversely, LV was non dilated with moderately reduced systolic function - LVEF 43%. There was paradoxical systolic motion of ventricle septum. The LV mass was 38g.

2.4. 2-Dimensional Color Echocardiography

Transthoracic color echocardiography exhibited multiple features as mentioned below:

- Levocardia
  - Situs solitus
  - Left aortic arch
  - Confluent pulmonary arteries
  - D- malposition of great arteries
  - SVC, IVC draining into the right lateral side of single atrium
  - 3 pulmonary veins draining into the left lateral side of single atrium
- Single atrium
  - No atrial septal tissue was identified.
- Common A-V orifice with a common A-V valve
- Ventricular septal defect - large, noncommitted (remote) VSD, with typical features of complete A-V canal defect (CAVD).
  - Size : 14 mm
  - Bidirectional shunt (Predominantly Lt to Rt.)
  - Rastelli Class A; There was extensive chordal attachment of single AV valve leaflets to the ventricular septal crux.
- Double outlet right ventricle
  - Both great arteries were totally arising from the morphologic RV.
- D - malposition of great arteries
  - Aorta was lying anterior and to the right of pulmonary artery
  - Pulmonary artery was lying posterior and to the left of aorta
  - Sub-aortic conus was present
- Pulmonary stenosis (severe)
  - PV domed.
  - Peak/mean gradient across PV 72/38 mmHg.
  - Hypoplasia of pulmonary valve annulus; dilated main-branch pulmonary arteries.

- PV annulus (D) 10 mm, MPA (D) 20 mm, LPA (D) 20 mm, RPA (D) 17.3 mm.

- Sub aortic stenosis (moderate)
  - A discrete obstructing membrane was present in the subaortic region.
  - Peak mean gradient across the membrane being 43.8/19.9 mmHg.
- AV valve regurgitation (severe)
  - Common AV valve was present
  - AV valve regurgitation peak velocity = 4.22 m/sec (peak gradient 71.3 mmHg)
  - On color flow mapping AV valve regurgitation jet area 32.07 sqcm; 70 % of single atrium area, central jet.
- Dilated RV with concentric hypertrophy, non dilated LV.
  - Normal RV systolic function RVEF = 55 %
  - Mildly reduced LV systolic function = 43 %
- Miscellaneous findings:
  - Mild circumferential pericardial effusion, large bilateral pleural effusion and moderate ascites were recognised.
- No evidence of COA, PDA, AS, anomalous pulmonary venous return.

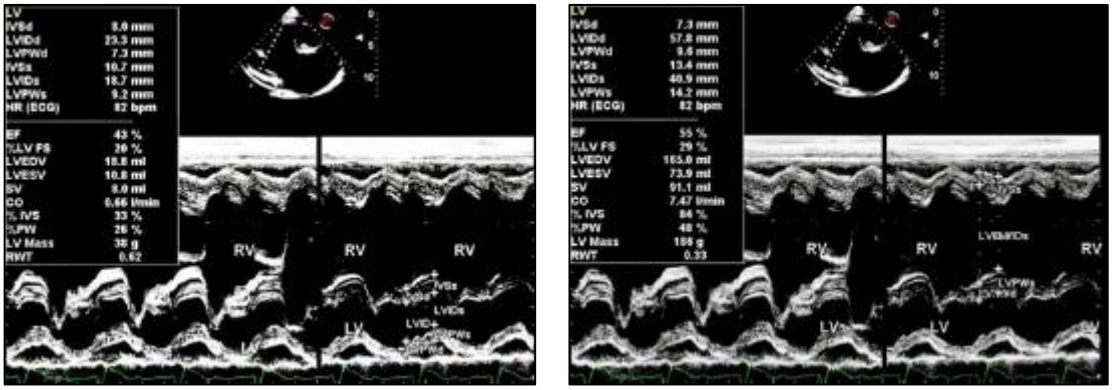

A B

Figure 11 M-mode Echocardiography. (A) LV and (B) RV, M-mode measurements

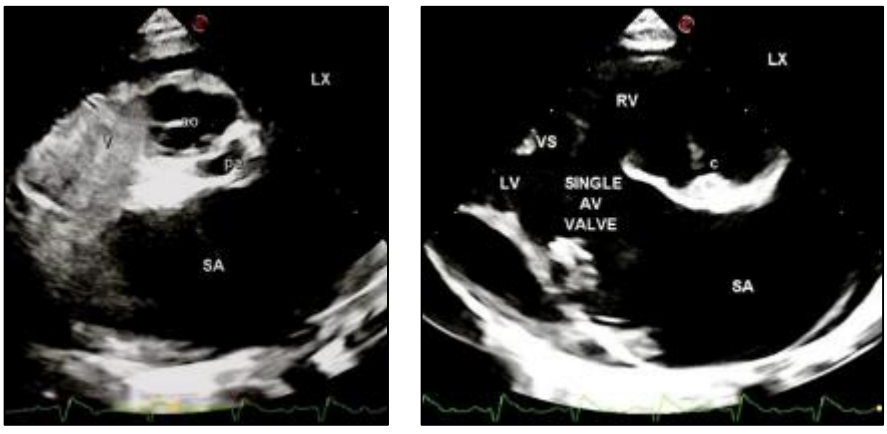

A B

Figure 12 Single atrium, common atrioventricular valve and D-transposition of great arteries. (A) In the LX view single atrium (SA) and great arteries are visualised; aorta (ao) is lying anterior and to the right of pulmonary artery (pa); (B) In another view of LX, a large single atrium, and a common AV valve overriding the ventricular septum (vs) was depicted. A subpulmonic conus (c) is distinctly identified

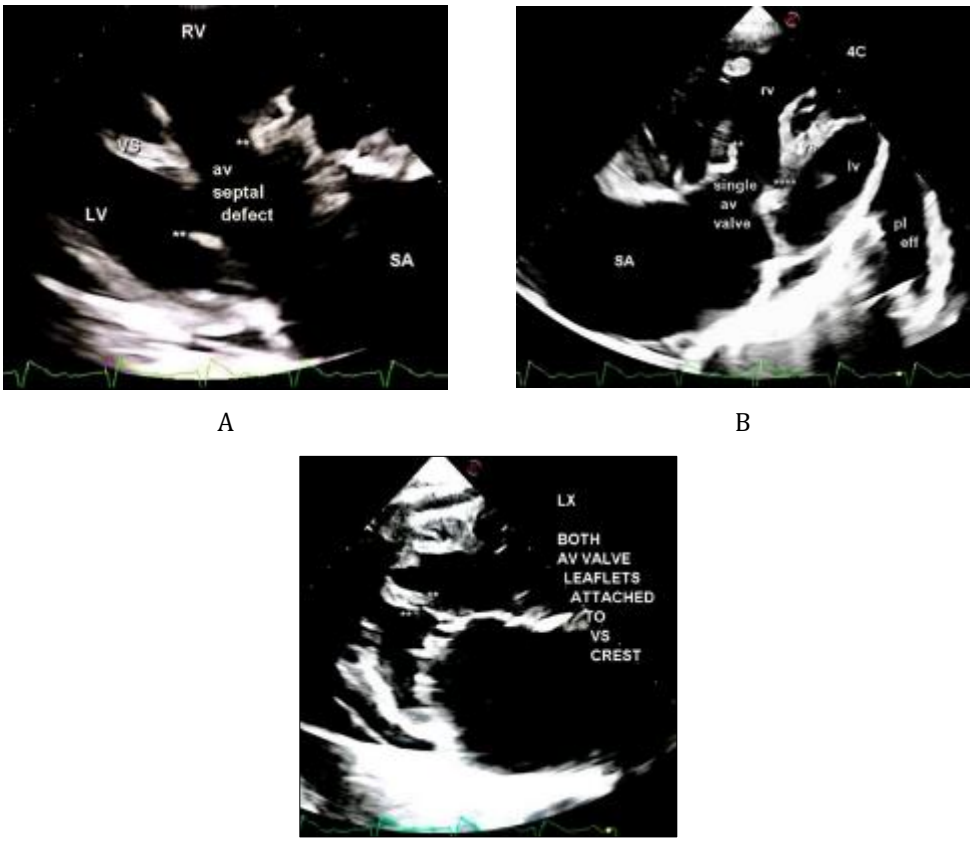

A B C

Figure 13 Noncommitted (remote) VSD with typical features of complete AV canal defect (CAVC). (A) In the LX view, a large av septal defect or CAVC was illustrated; (asterisk **) denotes common AV valve overriding the ventricular septum. SA, single atrium; VS, ventricular septum; (B) In the 4C view, a similar overriding of ventricular septum by common AV valve is shown. (asterisk **) is depicting the right lateral AV leaflet and (asterisk ****) is denoting the left lateral AV leaflet of the common AV valve; (C) In the LX view, common AV valve leaflets are seen attached to the ventricular septal crux (asterisk **)

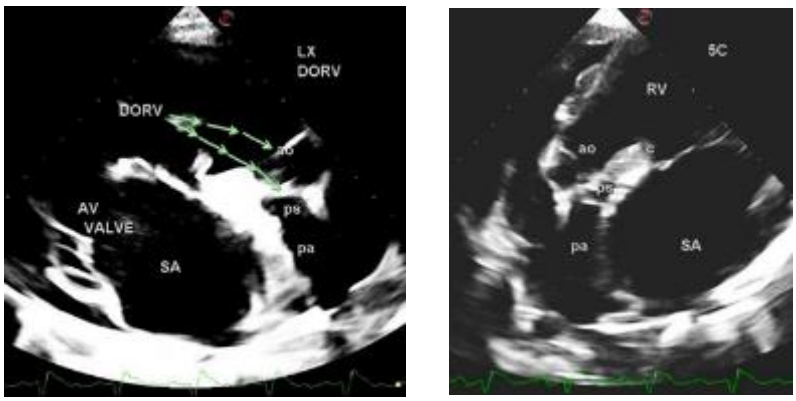

A B

Figure 14 (A) In the LX view, both the great arteries are arising totally from the morphological RV (DORV) . Moreover, there is d-transposition of great arteries (d-TGA) ; aorta (ao) is lying anteriorly and to the right of pulmonary artery (pa) and pa is lying posteriorly and to the right of ao; (B) Likewise, in the 5CH view the spatial relationship of d-tga is exemplified

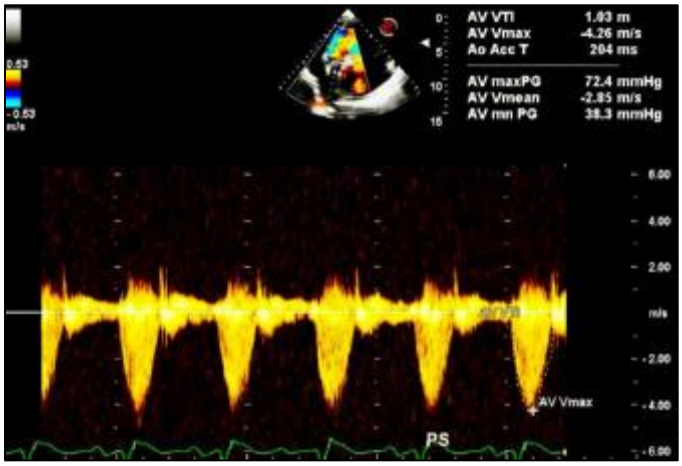

Figure 15 On continuous wave doppler (CWD) analysis across the pulmonary valve a CWD signal of severe pulmonary stenosis is displayed with a peak and mean gradient of 72.3/ 38.3 mmHg

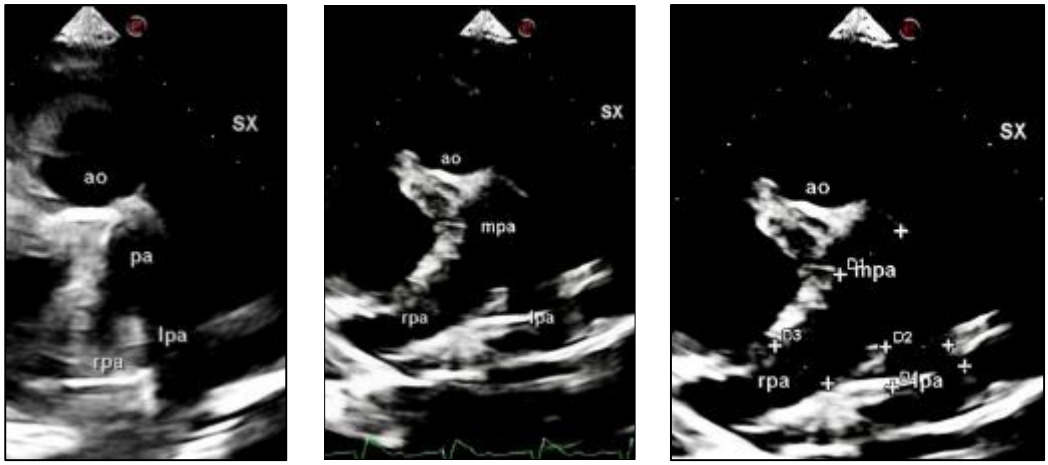

A B C

Figure 16 D-transposition of great arteries alongwith (A) hypoplasia of pulmonary valve (pv) annulus; (B, C) dilatation of main and branch pulmonary arteries: pv annulus (D) 7.3 mm, mpa (D) 20 mm, lpa (D) 20 mm, rpa (D) 17.3 mm

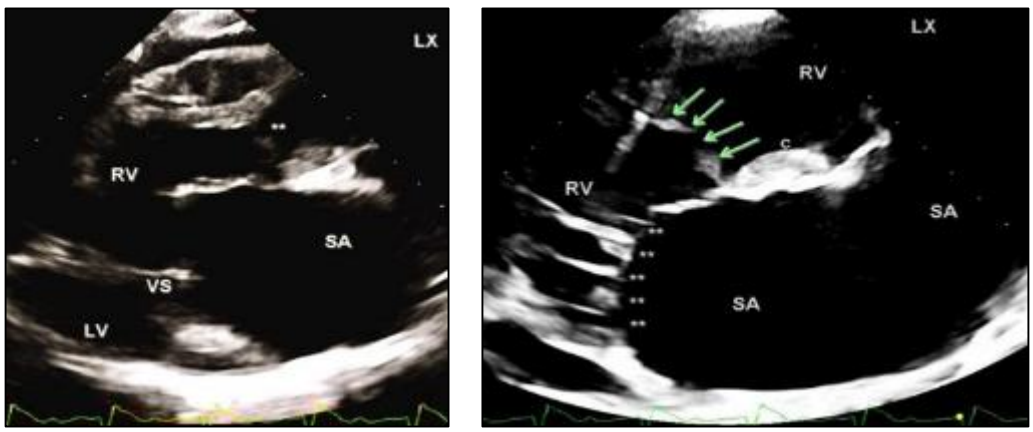

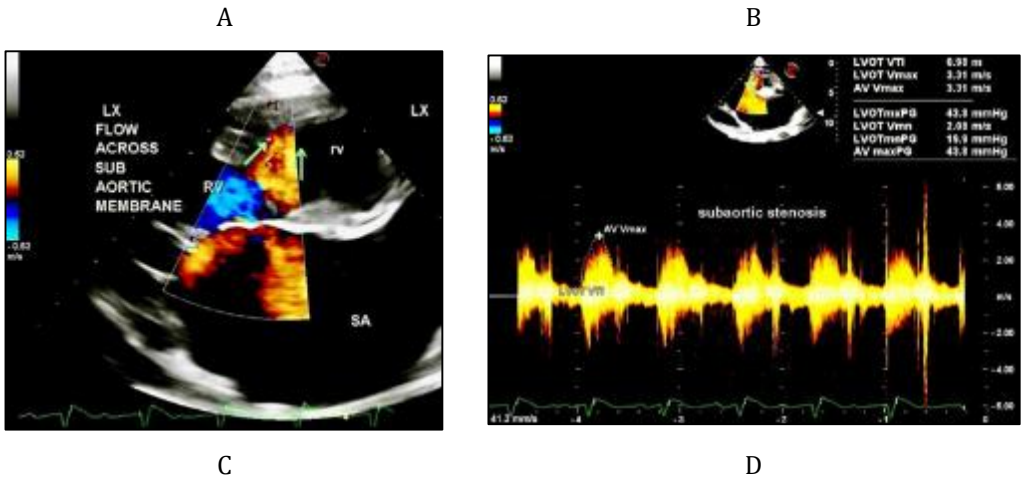

Figure 17 Subaortic stenosis. (A) In the LX view, large noncommitted (remote) VSD with typical features of complete AV canal defect is clearly outlined. The common AV valve was overriding the ventricular septum. Subaortic membrane is denoted by asterisk **; (B) In the LX view, a notable subaortic membrane is visualised (depicted by arrows) with a subaortic conus (c) and closed common AV valve (asterisk **); (C) on color flow imaging a turbulent pattern is seen in the subaortic region (arrows); (D) On CWD analysis across subaortic membrane a peak/mean gradient of 43.8/19.9 mmHg was present, consistent with moderate subaortic obstruction

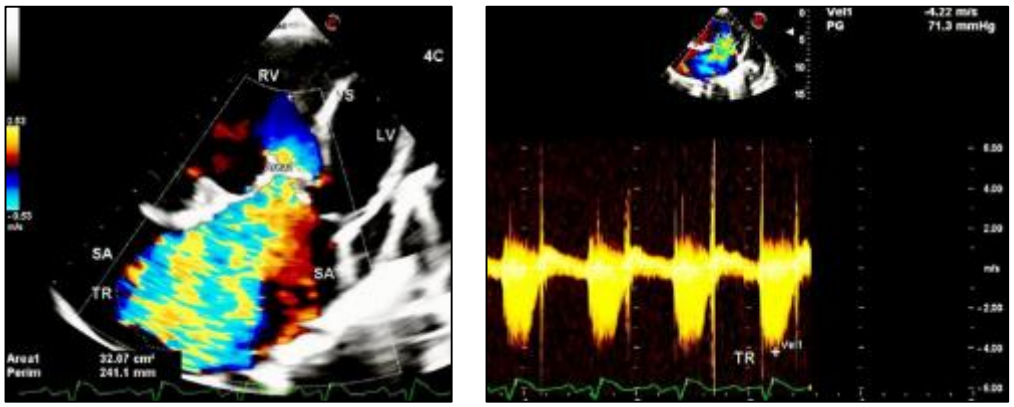

Figure 18 AV valve regurgitation (severe). (A) In the 4CH view, on color flow mapping (CFM), a striking mosaic pattern, turbulent jet of AV valve regurgitation is demonstrated in the single atrium (SA). The area of the jet was 32.07 sqcm, which was occupying approximately 70 % of single atrium area; (B) On continuous wave doppler (CWD) analysis across the AV valve, a peak velocity of AV valve regurgitation was 4.22 m/sec with a peak gradient of 71.3 mmHg

2.5. Summary of 2-Dimensional echocardiography findings

On transthoracic color echocardiography there was presence of single atrium, common A-V orifice, common A-V valve, large non-committed (remote) VSD with features of complete A-V canal defect- Rastelli Type A, DORV, D-transposition of great arteries, pulmonary valvular stenosis (severe), subaortic stenosis (moderate) and severe A-V valve regurgitation.

The right ventricle was dilated with normal RV systolic functioning. Conversely, LV was non-dilated with moderately reduced LV systolic function.

2.6. Future course of action

Because of severe affliction with complex cyanotic congenital heart disease our index patient was deeply cyanotic, breathless and in severe CHF. We advised the adolescent appropriate medical therapy according to the current

guidelines and suggested the parents to consult a tertiary care pediatric cardiovascular institute for a suitable palliative/corrective surgery.

3. Discussion

Double outlet right ventricle (DORV) is a heterogeneous group of abnormal ventriculoarterial connections where, by definition, both great arteries (pulmonary artery and aorta) arise primarily from the morphologically right ventricle.

It is a rare condition, affecting 1-1.5% of the patients with congenital heart diseases and occurring in 1 out of 10,000 live births [28].

Multiple classifications of DORV have been described by various authors, besides the one mentioned earlier by Peixoto et al [6]. Some important categorisations are mentioned here:

Table 4 DORV categories by Van Praagh [5]

Type I DORV as an isolated conotruncal anomaly
Type II DORV with conotruncal anomalies and associated malformations of the atrioventricular valve(s) and ventricles
Type III DORV associated with heterotaxy

Table 5 DORV categories by Lev et al [4]

1. With subaortic VSD Without pulmonary stenosis With pulmonary stenosis 2. With subpulmonic VSD Without pulmonary stenosis With pulmonary stenosis 3. With doubly committed VSD 4. With noncommitted VSD 5. Complicated types • With total anomalous pulmonary venous drainage • With common AV orifice or ostium primum defect i. With pulmonary stenosis ii. With aortic hypoplasia • With mitral atresia or stenosis i. With pulmonary stenosis Without VSD With VSD ii. With aortic stenosis or hypoplasia Without VSD With VSD • Combined complicated type
Legend: VSD, Ventricular septal defect. AV, Atrioventricular.

Modified Fuwai classification proposed by Pang et al [29] after analysis of 500 patients with DORV is based on three parameters namely great artery relation, location of the VSD, and presence of outflow obstruction. These parameters determine the clinical features and guide surgery (Table 6).

Table 6 Modified Fuwai classification with double-outlet right ventricle adapted from Pang, et al [29].

DORV subtypes	Relative position of great arteries	Relation between GA and VSD	RVOTO
IA	Normal	Committed	Absent
IB	Normal	Committed	Present
IIA	Normal	Non committed	Absent
IIB	Normal	Non committed	Present
IIIA	Abnormal	Committed	Absent
IIIB	Abnormal	Committed	Present
IVA	Abnormal	Non committed	Absent
IVB	Abnormal	Non committed	Present
DORV: Double-outlet right ventricle. VSD: ventricular septal defect, RVOTO: Right ventricular outflow tract obstruction.			

A more clinically relevant classification of DORV for anesthesiologist is that proposed by the Society of Thoracic Surgeons and the European Society for Thoracic Surgery, which classifies DORV into five different subtypes (PS= pulmonic stenosis) (Spaeth 2014 [30]; Lacour-Gayet 2008 [31]):

- VSD type: DORV with subaortic or doubly committed VSD (no PS)
- TOF type: DORV with subaortic or doubly committed VSD and PS
- TGA type: DORV with subpulmonary VSD (with or without PS)
- Remote VSD type: DORV with a remote VSD (with or without PS)
- DORV and AVSD

This classification allows for better conceptualization and understanding of physiologic and surgical goals.

The most prevalent anatomic arrangement observed in DORV is that of normally committed great arteries, i.e., posterior and right-sided aorta, with subaortic VSD and subpulmonary stenosis. Then, from the highest to the lowest frequency, it is followed by subaortic VSD without pulmonary obstruction, doubly-committed or non-committed VSD, and the extremely rare subpulmonary VSD [32, 33].

The most frequently found VSD is the subaortic, although it can be doubly-commited, subpulmonary or non-commited [6, 32, 33].

The additional malformations most frequently encountered in DORV are: 1) when the VSD is subaortic: subpulmonary stenosis; 2) when the VSD is subpulmonary: subaortic stenosis, coarctation and interruption of the aortic arch, overriding and bilateral insertion of the mitral valve cusps; 3) with any kind of VSD: atrial septal defect, patent ductus arteriosus and juxtaposition of the atrial appendages; and 4) with non-committed VSD: atrioventricular septal defect, overriding and bilateral insertion of the tricuspid valve [6].

2-dimensional echocardiography has significantly contributed to the diagnosis and knowledge of the anatomic variations of DORV through the accurate assessment of the intracardiac abnormalities, many times making hemodynamic studies unnecessary, except in cases where a total surgical correction is suggested [28, 33].

The wide spectrum of anatomic variations found in DORV may result in different clinical findings and require different therapeutic approaches.

Aoki et al [34] reported one of the largest case series of DORV. In 10 years, 73 patients underwent heart surgery for correction of different types of DORV. A large majority of patients, the aorta and the pulmonary trunk were side by side, 18 (25%) showed a posterior and right-sided aorta, 12 (17%) showed an anterior and right-sided aorta, 5 (7%) showed an anterior and left-sided aorta, and only 2 (2.8%) showed an anterior aorta.

3.1. Non-committed (or remote) ventricular septal detect

The term 'non-committed' (or remote) was used to define hearts in which the ventricular septal defect (VSD) was anatomically related to, or was close to, neither great vessel, being separated from both by considerable muscle. DORV with non-committed VSD has challenged surgeons throughout the modern era of congenital heart surgery [35-37]. This subset was known to have a poor outcome and higher risk for reoperation, and was frequently treated by an univentricular repair [38].

3.2. Anatomic considerations of non-committed ventricular septal detect

Non-committed is not an anatomic definition: it was used to define the location of the VSD in cases with DORV in which the VSD was distant from both arterial valves [2]. This subset includes DORV with an atrioventricular (AV) canal type, inlet (muscular) or trabecular VSD. Also, it exits as DORV with conoventricular (perimembraneous) VSD distant to the great arteries because of the length of the subarterial conus.

The term non-committed was first used by Lev et al. in 1972 [4]. In 1975, Zamora, Moller and Edwards employed the term 'remote' to define these defects [39]. Van Praagh et al. also used the term 'uncommitted' [5]. Both terms were used to describe the presence of a 'considerable' distance between the VSD and the outflow tracts supporting the aorta and the pulmonary trunk rather than being anatomical definitions. Thus, this subgroup of DORV included patients with AV canal type VSD, with trabecular VSD (inlet or not), but also patients with conoventricular VSD distant to the arterial valves.

4. Conclusion

Despite rarity, DORV should be considered in the differential diagnoses of patients presenting with generalised cyanosis since birth. Early recognition and prompt management may improve outcomes in such patients.

Echocardiography is an effective and extremely useful method for diagnosing this complex malformation. This test accurately identifies the anatomical variables and guides the choice of the most appropriate surgical approach.

Compliance with ethical standards

Disclosure of conflict of interest

No conflict of interest to be disclosed.

Statement of ethical approval

Ethical approval was obtained from the ethics review committee of Prakash Heart Station, Niralanagar, Lucknow.

Statement of informed consent

Informed consent was procured from the parents of the adolescent male.

References

[1] Mery: Diverses observations anatomiques. Histoire de I' Acad., Royal des Sciences, Paris, 1703, p. 42 (obsevation 42).

[2] Braun K, De Vries A, Feingold DS, Ehrenfeld NE, Feldman J, Schorr S. Complete dextroposition of the aorta, pulmonary stenosis, interventricular septal defect, and patent foramen ovale. Am Heart J 1952, 43:773-80.

[3] Witham AC. Double outlet right ventricle, a partial transposition complex. Am Heart J 1957, 53:928-39.

[4] Lev M, Bharati S, Meng CC, Liberthson RR, Paul MH, Idriss F. A concept of double- outlet right ventricle. J Thorac Cardiovasc Surg 1972, 64:271-81.

[5] Van Praagh S, Davidoff A, Chin A, Shiel F, Reynolds J, Van Praagh R. Double outlet right ventricle: anatomic types and developmental implications based on a study of 101 autopsied cases. Coeur. 1982, 13:389-439.

[6] Peixoto LB, Leal SM, Silva CE, Moreira SM, Ortiz J. Double outlet right ventricle with anterior and left-sided aorta and subpulmonary ventricular septal defect. Arq Bras Cardiol. 1999, 73:441-50.

[7] Walters HL, Mavroudis C, Tchervenkov CI, Jacobs JP, Lacour-Gayet F, Jacobs ML. Congenital Heart Surgery Nomenclature and Database Project: double outlet right ventricle. Ann Thorac Surg 2000, 69:249-63.

[8] Baciewicz FA Jr, Melvin WS, Basilius D, Davis JT. Congenital heart disease in Down's syndrome patients: a decade of surgical experience. Thorac Cardiovasc Surg 1989, 37:369-71.

[9] Brown DL, Emerson DS, Shulman LP, Doubilet PM, Felker RE, Van Praagh S. Predicting aneuploidy in fetuses with cardiac anomalies: significance of visceral situs and noncardiac anomalies. J Ultrasound Med 1993, 12:153-61.

[10] Bruyere HJ, Kargas SA, Levy JM. The causes and underlying developmental mechanisms of congenital cardiovascular malformations: a critical review. Am J Med Genet Suppl 1987, 3:411-31.

[11] Fyler DC. Double-outlet right ventricle. Nadas' pediatric cardiology. Philadelphia: Hanley and Belfus, 1992:643-8.

[12] Hagler DJ. Double outlet right ventricle. In: Allen, Driscoll, Shaddy, Feltes, eds. Moss and Adams heart disease in infants, children, and adolescents including the fetus and young adult, 7 ed. Philadelphia: Lippincott, Williams and Wilkins, 2008:1100-27.

[13] Jones KL. Smith's recognizable patterns of human malformations, 5 ed. Philadelphia: WB Saunders Co, 1997.

[14] Lin AE. Congenital heart defects in malformation syndromes. Clin Perinatol 1990, 17:641-73.

[15] Botto LD, Correa A. Decreasing the burden of congenital heart anomalies: an epidemiologic evaluation of risk factors and survival. Prog Pediatr Cardiol 2003, 18:111-21.

[16] Loffredo CA. Epidemiology of cardiovascular malformations: prevalence and risk factors. Am J Med Genet 2000, 97:319-25.

[17] Pradat P, Francannet C, Harris JA, Robert E. The epidemiology of cardiovascular defects, part 1: a study based on data from three large registries of congenital malformations. Pediatr Cardiol 2003, 24:195-221.

[18] Hoffman JI, Kaplan S. The incidence of congenital heart disease. J Am Coll Cardiol 2002, 39:1890-900.

[19] Silka MJ. Double-outlet right ventricle. Oski's pediatrics: principles and practice. Philadelphia: Lippincott, Williams, and Wilkins, 1999:1332-4.

[20] Chen SJ, Lin MT, Liu KL, Chang CI, Chen HY, Wang JK, et al. Usefulness of 3D reconstructed Computed tomography imaging for double outlet right ventricle. J Formos Med Assoc. 2008, 107:371-380.

[21] Dydynski PB, Kiper C, Kozik D, Keller BB, Austin E, Holland B. Three-dimensional reconstruction of intracardiac anatomy using CTA and surgical planning for double outlet right ventricle: early experience at a tertiary care congenital heart center. World J Pediatr Congenit Heart Surg. 2016, 7:467-474.

[22] Priya S, Nagpal P, Sharma A, Pandey NN, Jagia P. Imaging spectrum of double-outlet right ventricle on multislice computed tomography. J Thorac Imaging. 2019, 34:W89-W99.

[23] Garekar S, Bharati A, Chokhandre M, Mali S, Trivedi B, Changela VP, et al. Clinical application and multidisciplinary assessment of three dimensional printing in double outlet right ventricle with remote ventricular septal defect. World J Pediatr Congenit Heart Surg. 2016, 7:344-350.

[24] Bhatla P, Tretter JT, Chikkabyrappa S, Chakravarti S, Mosca RS. Surgical planning for a complex double-outlet right ventricle using 3D printing. Echocardiography. 2017, 34:802-804.

[25] Yoo SJ, van Arsdell GS. 3D printing in surgical management of double outlet right ventricle. Front Pediatr. 2018, 5:289.

[26] Yim D, Dragulescu A, Ide H, Seed M, Grosse-Wortmann L, van Arsdell G, et al. Essential modifiers of double outlet right ventricle: revisit with endocardial surface images and 3-dimensional print models. Circ Cardiovasc Imaging. 2018, 11:e006891.

[27] Goo HW, Park SJ, Yoo SJ. Advanced medical use of three-dimensional imaging in congenital heart disease: augmented reality, mixed reality, virtual reality, and three-dimensional printing. Korean J Radiol. 2020, 21:133–145.

[28] Silka MJ. Double outlet right ventricle. In: Garson A, Bricker JT, Fisher DJ, Neish SR - The Science in Practice of Pediatric Cardiology. 2nd ed. Willians & Wilkings, 1998:1505-23.

[29] Pang KJ, Meng H, Hu SS, Wang H, Hsi D, Hua ZD, et al. Echocardiographic classification and surgical approaches to double-outlet right ventricle for great arteries arising almost exclusively from the right ventricle. Tex Heart Inst J 2017, 44:245-51.

[30] Spaeth JP. Perioperative Management of DORV. Semin Cardiothorac Vasc Anesth. 2014, 18:281-9.

[31] Lacour-Gayet F. Intracardiac repair of double outlet right ventricle. Seminars in thoracic and cardiovascular surgery. Pediatric cardiac surgery annual. 2008, 39-43.

[32] Anderson RH, Becker AE. Abnormal ventriculo-arterial connexions. In: Cardiac Pathology. An Integrated Text and Colour Atlas. 1st ed. London: Churchill Livingstone, 1983:14-1.

[33] Freedon R, Smallhorn J. Double outlet right ventricle. In: Freedon R, Benson L, Smallhorn J - Neonatal Heart Disease. 1st ed. London: Springer Verlag, 1992:453-70.

[34] Aoki M, Forbess JM, Jonas RA, Mayer Jr JE, Castaneda A. Result of biventricular repair for double outlet right ventricle. J Thorac Cardiovasc Surg 1994, 107:338-50.

[35] Kirklin JW, Pacifico AD, Blackstone EH, Kirkim JK, Bargeron LM. Current risks and protocols for operations for double-outlet right ventricle: derivation from an 18 year experience. J Thorac Cardiovasc Surg 1986, 92:913-930.

[36] Kleinert S, Sano T, Weintraub RG, Mee RBB, Karl T, Wilkinson JL. Anatomic features and surgical strategies in double-outlet right ventricle. Circulation 1997, 9:1233-1239.

[37] Stellin G, Ho SY, Anderson RH, Zuberbuhler JR, Siewers RD. The surgical anatomy of double-outlet right ventricle with concordant atrioventricular connection and noncommitted ventricular septal defect. J Thorac Cardiovasc Surg 1991, 102:849-855.

[38] Freedom RM, Van Arsdell GS. Biventricular hearts not amenable to biventricular repair. Ann Thorac Surg 1998, 66:641-643.

[39] Zamora R, Moller JH, Edwards JE. Double outlet right ventricle: anatomic types and associated anomalies. Chest 1975, 68:672-677.